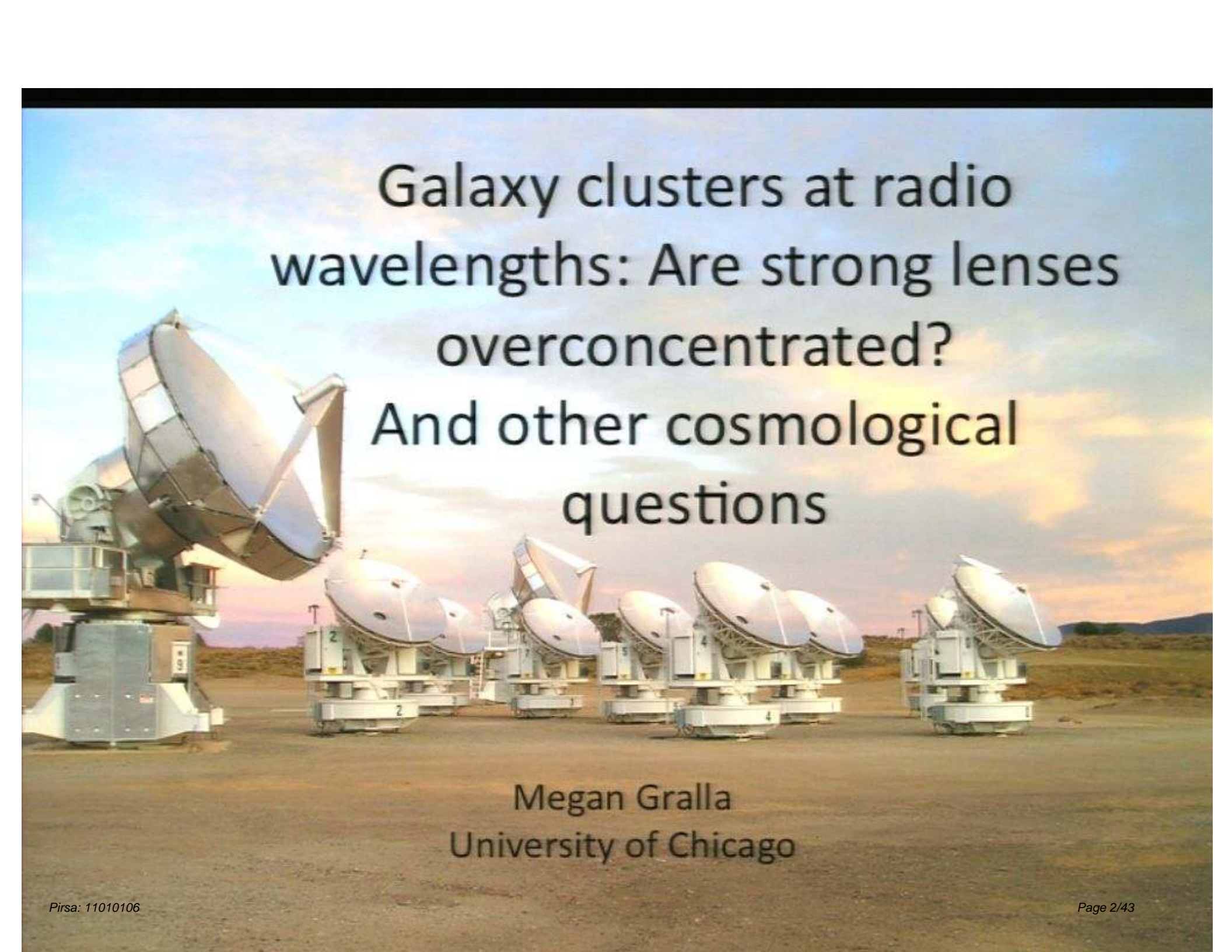


Title: Galaxy clusters at radio wavelengths: Are strong lenses overconcentrated? And other cosmological questions

Date: Jan 18, 2011 02:00 PM

URL: <http://pirsa.org/11010106>

Abstract: Strong lensing galaxy clusters provide promising probes of cosmological structure formation. Strong lensing halos can be identified in cosmological simulations through ray tracing techniques and their properties measured. Previous studies have found some evidence that strong lensing clusters are more concentrated than expected, with possible explanations including baryonic effects or more exotic physics such as early dark energy. Using Sunyaev-Zeldovich (SZ) observations to measure the mass on large scales and strong lensing mass modeling for small scales, we find that the clusters are more concentrated than expected at the 97% confidence level. We also investigate the placement of lensed images with respect to the SZ gas and Brightest Cluster Galaxy orientations. I will also discuss the redshift evolution of radio Active Galactic Nuclei in clusters, which is relevant for determining cosmological parameters from SZ surveys as well as for understanding the energy budgets in cluster cores.

A photograph of several large radio telescope dishes in a desert landscape under a sunset sky. The dishes are arranged in a line, and the sky is a mix of blue, orange, and yellow. The text is overlaid on the right side of the image.

Galaxy clusters at radio
wavelengths: Are strong lenses
overconcentrated?
And other cosmological
questions

Megan Gralla
University of Chicago

Collaborators

Mike Gladders

Keren Sharon

Ben Koester

Matt Bayliss

Felipe Barrientos

Howard Yee

David Gilbank

Masamune Oguri

John Carlstrom

Dan Marrone

Tom Plagge

Tom Culverhouse

Chris Greer

Ryan Hennessy

Marshall Joy

Max Bonamente

Nicole Hasler

Esra Bulbul

Stephen Muchovej

Tony Mroczkowski

Amber Miller

Dave Woody

Dave Hawkins

James Lamb

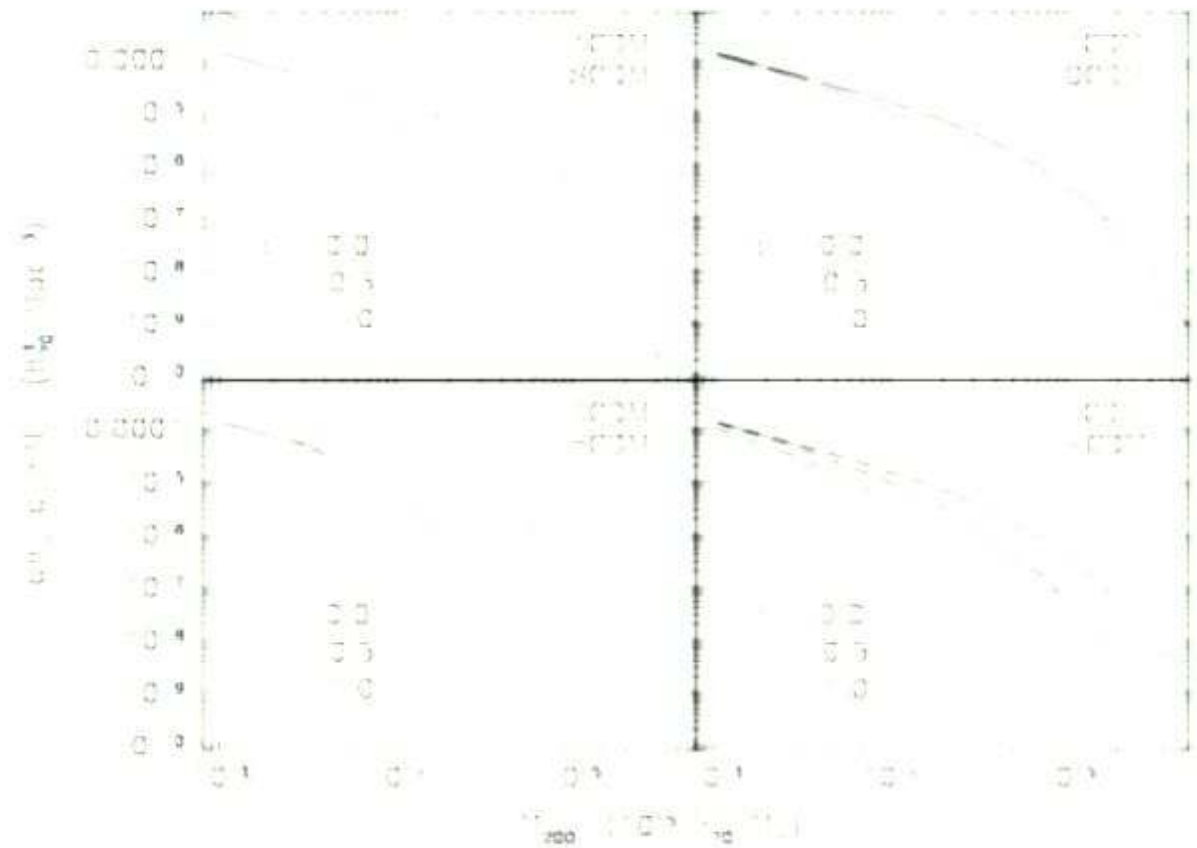
Galaxy Clusters Primer

Galaxy cluster content by mass



- Dark Matter
- Gas
- Galaxies

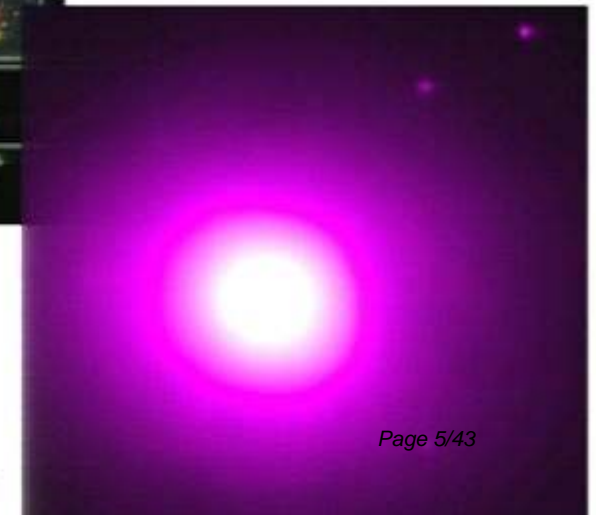
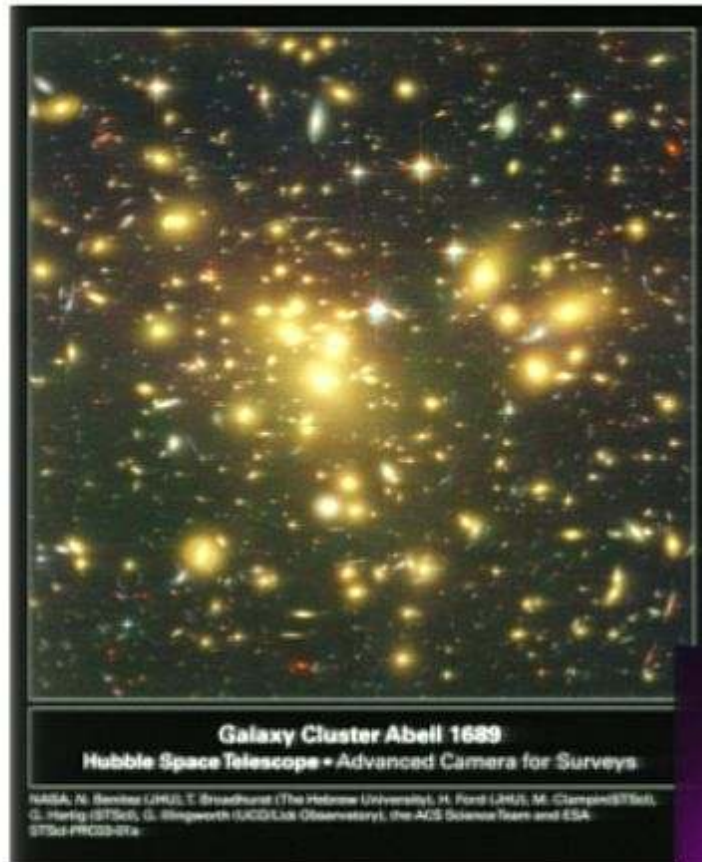
Useful for Cosmology: Trace the Growth of Structure



Voit 2004

Galaxy Cluster Mass Observables

- Optical
 - Richness
 - Velocity dispersion
 - Strong lensing
 - Weak lensing
- X-ray
 - Luminosity
 - Temperature
- Sunyaev Zel'dovich Effect



Sunyaev Zel'dovich (SZ) Effect

Spectral distortion in CMB caused by the scattering of CMB photons off of high energy electrons in the intracluster medium (ICM)

References: Sunyaev & Zel'dovich 1970, 1972; see also Birkinshaw 1999

SZ Effect:

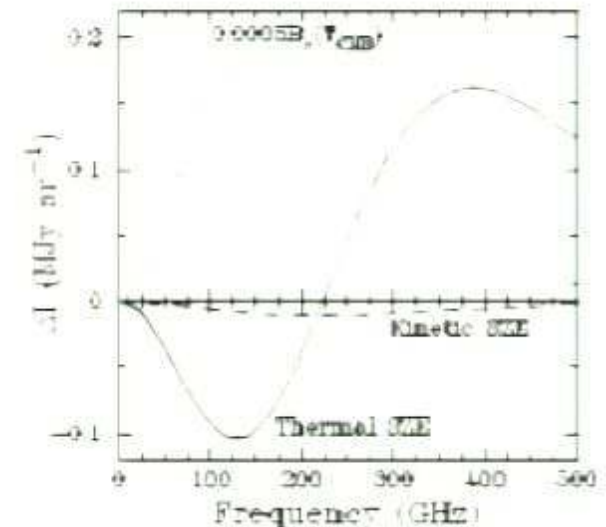
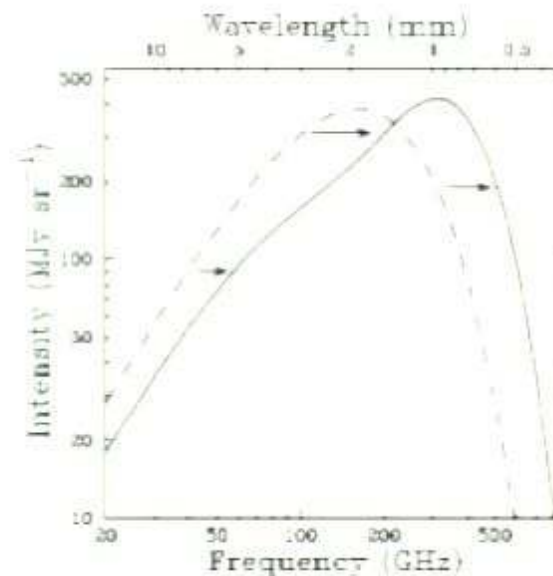
$$\frac{\Delta I_{SZE}}{I_{CMB}} = f(x) y = f(x) \int n_e \frac{k_B T_e}{m_e c^2} \tau_T dV$$

$$f(x) = \left(x \frac{x^2 + 1}{x^2 - 1} - 4 \right) \left[1 + \delta_{SZE}(x, T_e) \right]$$

$$x = \frac{h\nu}{m_e c^2}$$

Integrated Compton y-parameter

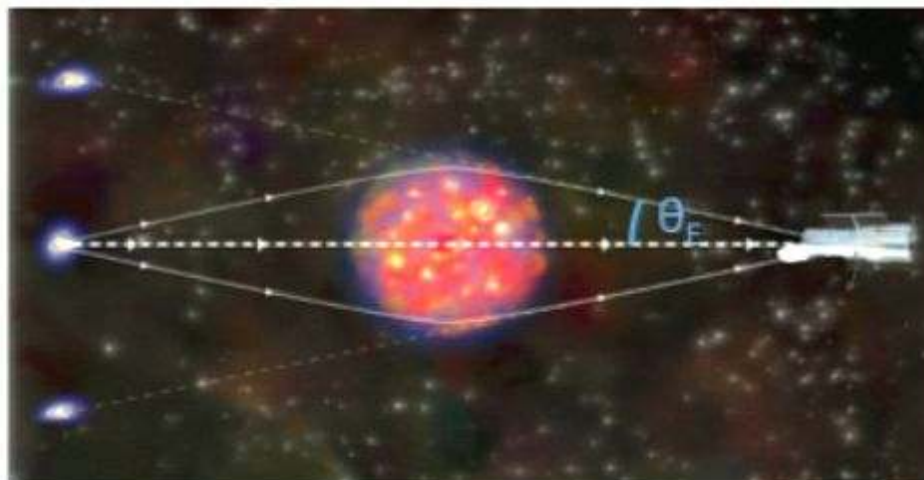
$$\int \Delta I_{SZE} d\Omega \propto \frac{N_e T_e}{D_A^2} \propto \frac{M T_e}{D_A^2}$$



Carlstrom, Holder & Reese (2002)

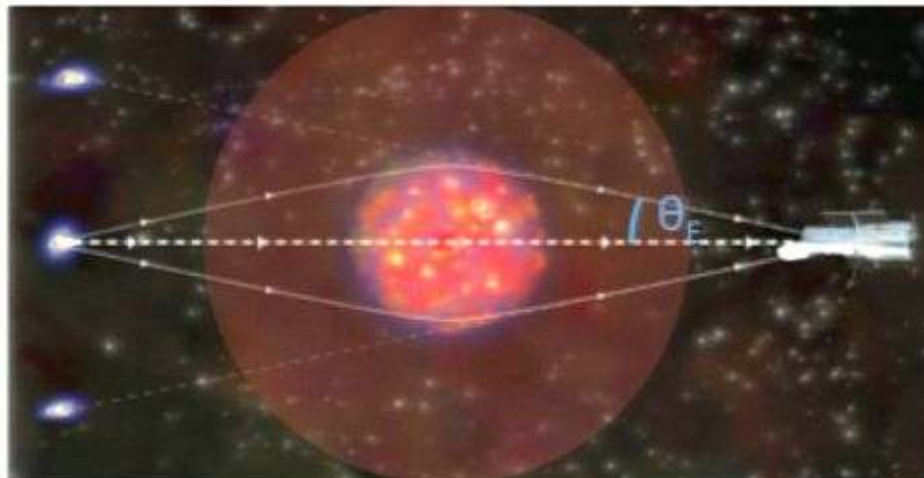
Strong Lensing

- Strong lensing occurs (multiple images can form) when the surface mass density exceeds the critical surface $\Sigma_{\text{cr}} = \frac{c^2}{4\pi G} \frac{D_s}{D_d D_{ds}} = 0.35 \text{ g cm}^{-2} \left(\frac{D}{1 \text{ Gpc}} \right)^{-1}$
- The Einstein radius is defined for a circularly symmetric mass distribution by $\theta_E = \left[\frac{4GM(\theta_E)}{c^2} \frac{D_{ds}}{D_d D_s} \right]^{1/2}$



Strong Lensing

- Strong lensing occurs (multiple images can form) when the surface mass density exceeds the critical surface $\Sigma_{cr} = \frac{c^2}{4\pi G} \frac{D_s}{D_d D_{ds}} = 0.35 \text{ g cm}^{-2} \left(\frac{D}{1 \text{ Gpc}} \right)^{-1}$
- The Einstein radius is defined for a circularly symmetric mass distribution by $\theta_E = \left[\frac{4GM(\theta_E)}{c^2} \frac{D_{ds}}{D_d D_s} \right]^{1/2}$



Cosmology with strong lenses

- Strong lenses can also be used to measure the Hubble constant through time delays (as proposed by Refsdal 1964) and to study the typically faint but highly magnified background source population
- Cluster scale strong lenses probe the tail of the distribution of clusters, sampling the most massive collapsed objects
- Dark matter halos that make good strong lenses can be robustly identified in simulations through ray-tracing techniques, and their properties studied

Strong lensing selection

- Ingredients that increase the chance a given halo acts as a strong lens:
 - Mass
 - Concentration
 - Line of sight elongation
 - Substructure
 - BCG mass
 - Baryonic physics
 - Surrounding large scale structure

Strong lensing selection

- Ingredients that increase the chance a given halo acts as a strong lens:

- Mass

- Concentration

- Line of sight elongation

- Substructure

- BCG mass

- Baryonic physics

- Surrounding large scale structure

Hennawi et al. 2007

Meneghetti et al. 2007

Meneghetti et al. 2003

Rozo et al. 2008

Puchwein & Ewald 2009

A mismatch between theory and observations?

- Overconcentration problem:
 - Oguri et al. (2005) compared CDM predictions for halo triaxiality with A1689 lensing measurements: found 6% of cluster halos can match A1689 at 2σ
 - Hennawi et al. (2007) used simulations to predict average concentrations of lensing clusters. Observations of lenses indicated higher concentrations than predicted
 - Problem persists with larger samples: eg., Oguri et al. (2009)
 - But for the few clusters studied to date, this is disputed: eg., Limousin et al. (2008); Morandi et al. (2010)
- Broadhurst & Barkana (2008) recast this from concentration measurement to comparison between virial masses and core masses. They showed that observed Einstein radii for 4 well-studied clusters lie well beyond predicted distribution in the standard Λ -CDM cosmology

Possible Explanations for Mismatch

- Halos that form earlier tend to be more concentrated (Wecshler et al. 2002)
 - Early dark energy (Fedeli & Bartelmann 2007)
 - Primordial non-gaussianity (Mathis et al. 2004)
- Baryonic effects (e.g., Rozo et al. 2008; Dalal, Holder & Hennawi 2004)
- Shortcomings of the models (e.g., if redshift evolution of the concentrations of the most massive clusters is different than for lower mass clusters, Zhao et al. 2003)
- Systematics on mass determinations for strong lensing clusters
- Minimal understanding of sample population from which known strong lenses are drawn

Project 1: Are strong lensing clusters overconcentrated?

Method: Observe a statistically defined sample of strong lensing clusters with the SZA, using the SZ effect to measure the mass on large scales and strong lensing mass models to measure the mass on small scales. Combining the two probes the projected concentration.

Strong lensing sample

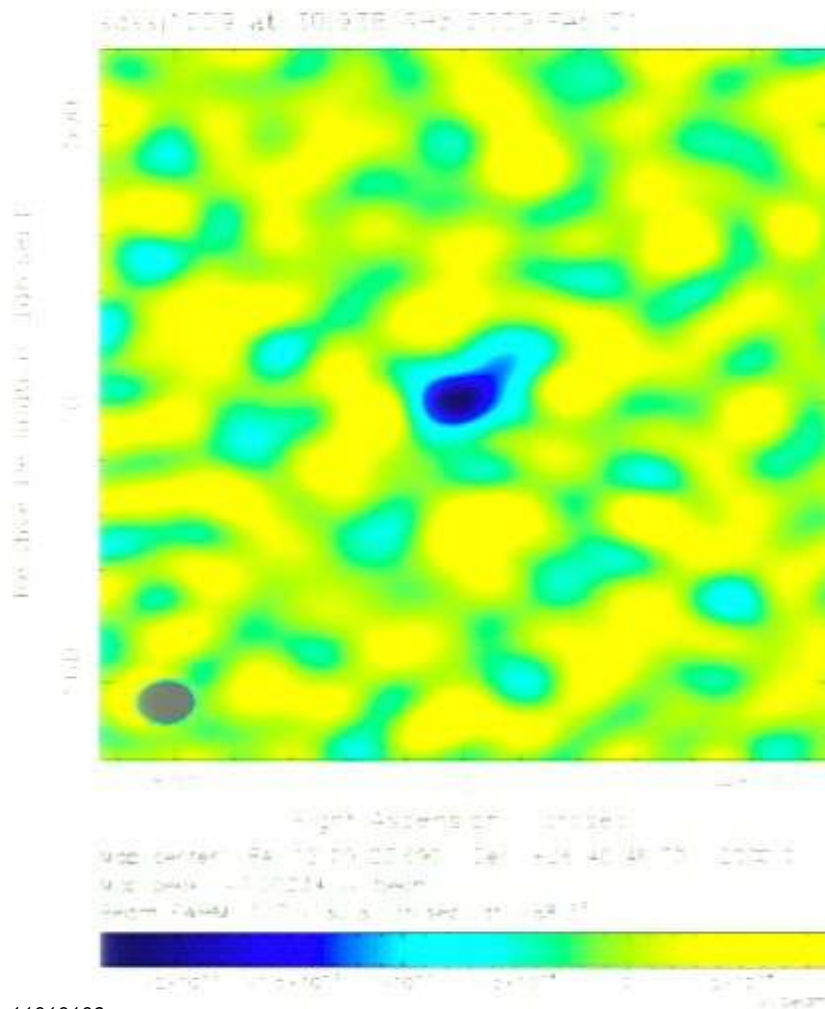
- Sloan Giant Arc Survey (SGAS; Hennawi et al. 2008) based on follow-up program of richest clusters in Sloan Digital Sky Survey (SDSS)
- Red-Sequence Cluster Survey (RCS; Gilbank et al. arXiv:1012.3470, Gladders et al. 2003) Giant Arcs based on survey imaging of RCS
 - Both taken from optically-selected clusters identified through red-sequence techniques (inclusive samples)
 - Lensing features identified visually, with selection characterized



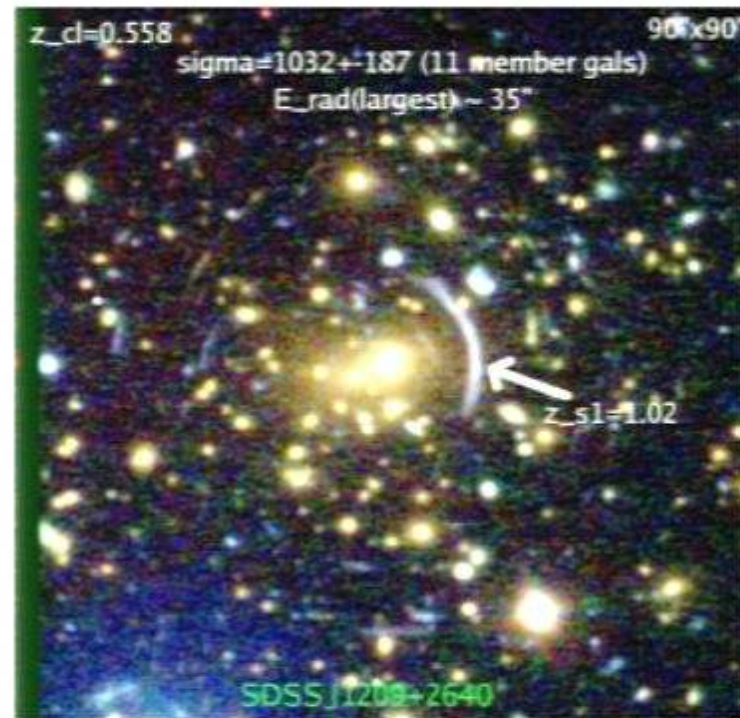
Sunyaev Zel'dovich Array (SZA)

- 8-element interferometer of 3.5 m antennas operating at 30 and 90 GHz, part of the Combined Array for Research in Millimeter-wave Astronomy (CARMA) located at Owens Valley Radio Observatory, CA.
- Typical observing configuration for cluster science has 6 antennas in compact configuration ($\sim 2'$ resolution) and 2 antennas further apart ($\sim 0.3'$ resolution) for simultaneous measurement of any contaminating unresolved radio sources.

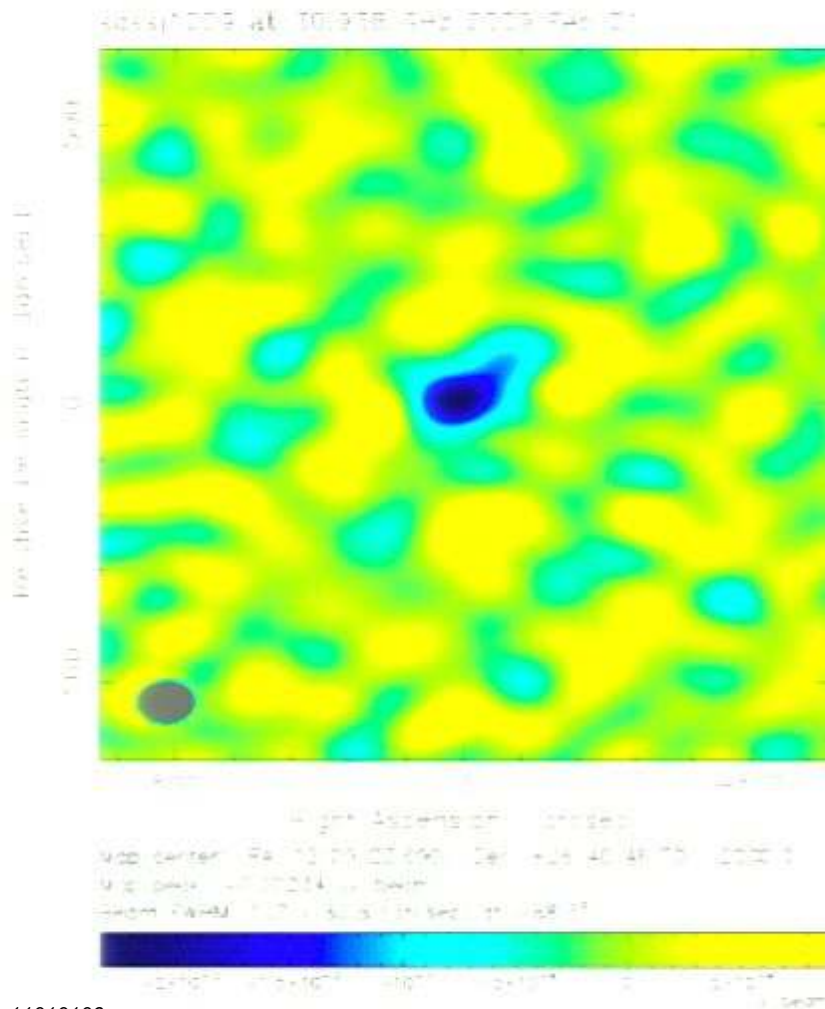
SZA observations of SDSSJ1209



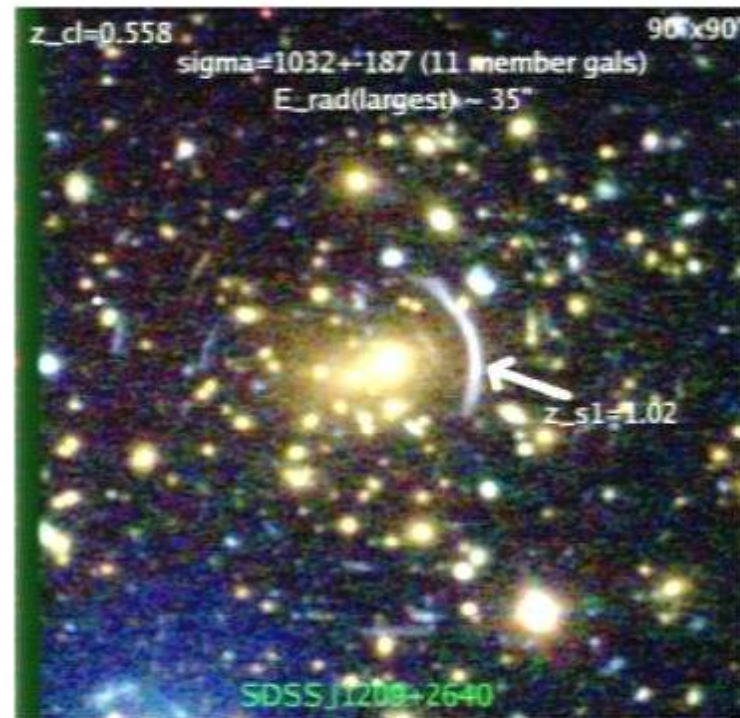
30 GHz SZ observations. 2 off-center point sources removed from map.

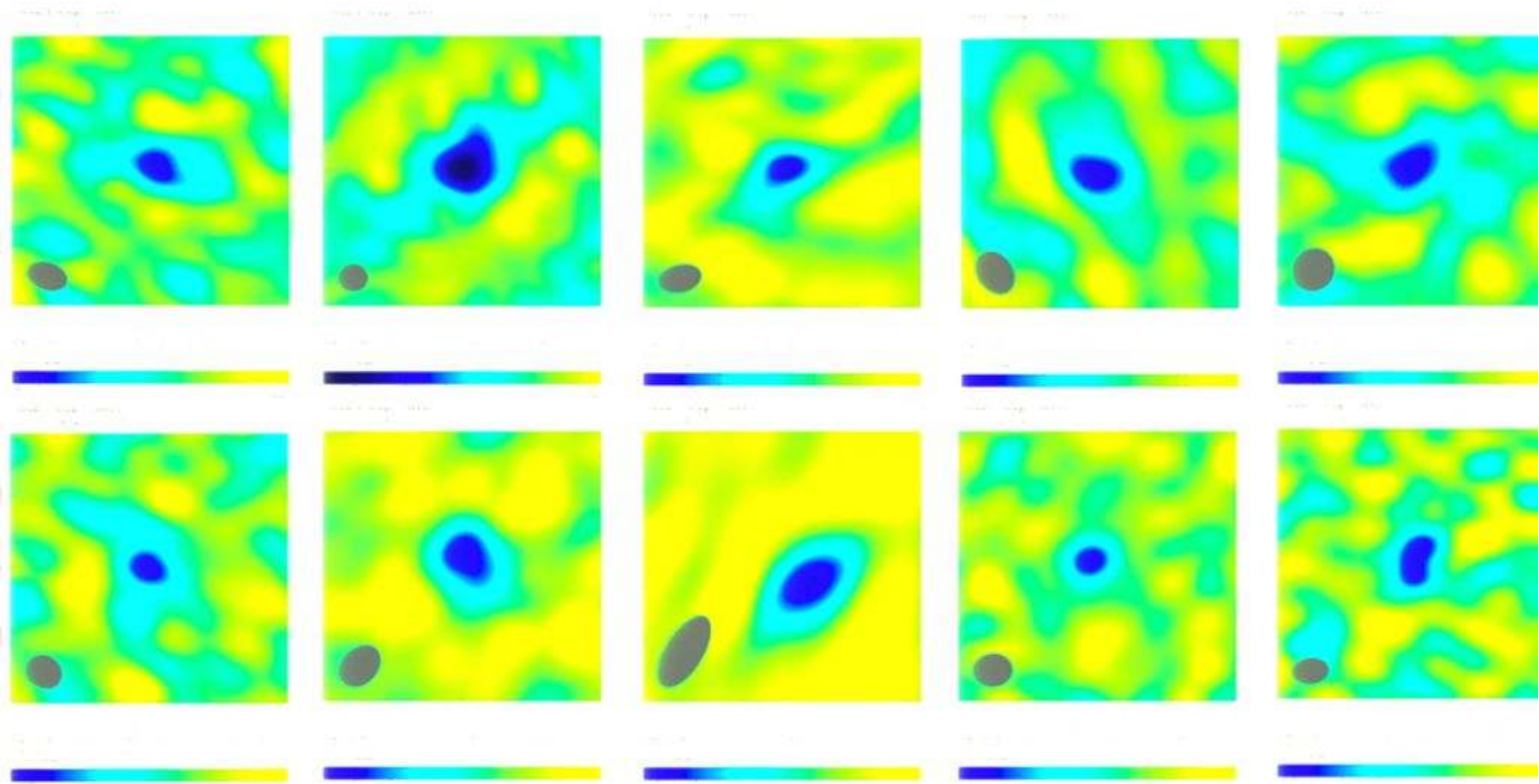


SZA observations of SDSSJ1209



30 GHz SZ observations. 2 off-center point sources removed from map.





SZ → Mass

- Fit model for pressure profile to interferometric data using MCMC analysis
- Calculate integrated Y
- Using scaling relation based on local sample, calculate mass

Strong Lensing Cluster Sample

Name	Cluster ID	z_s	z_l	V_{500} (10^3 Mpc 3)	M_{500} ($10^{14} M_{\odot}$)	Area (10^3 arcmin 2)	θ_s	θ_l	for lensing	for $z_{lens} < 2.0$	Lensing Ref.
A902-1689	18	0.6	23.8 $^{+0.1}_{-0.2}$	10.9 $^{+0.4}_{-0.5}$	1.00 $^{+0.05}_{-0.06}$	11.0	12.6	30.2 $^{+2.0}_{-2.1}$	-	-	-
A902-1703	18	2.1	16 $^{+1}_{-1}$	3.9 $^{+0.7}_{-0.8}$	0.88 $^{+0.10}_{-0.11}$	13.2	13.2	32.5 $^{+1.9}_{-2.0}$	2	-	-
A902-963	21	3.2	14 $^{+1}_{-1}$	3.0 $^{+0.5}_{-0.6}$	0.77 $^{+0.08}_{-0.09}$	16.7	16.5	8 $^{+1}_{-1}$	3	-	-
BCS1-22319	19	8 $^{+1}_{-1}$	2.1 $^{+0.1}_{-0.1}$	2.0 $^{+0.1}_{-0.1}$	1.86 $^{+0.10}_{-0.11}$	12.0	12.8 $^{+0.7}_{-0.8}$	25.3 $^{+1.6}_{-1.7}$	1	-	-
BCS2-22327	19	3.3	2.4 $^{+0.1}_{-0.1}$	2.7 $^{+0.1}_{-0.1}$	1.70 $^{+0.08}_{-0.09}$	21.8	21.8	25.3 $^{+1.6}_{-1.7}$	1	-	-
BCS2-22327	17	1.5	12.3 $^{+0.7}_{-0.8}$	6.1 $^{+0.8}_{-0.9}$	1.15 $^{+0.10}_{-0.11}$	25.9	25.9	31.1 $^{+1.7}_{-1.8}$	3	-	-
SDSS J1255-29	19	1.1	7.3 $^{+0.7}_{-0.8}$	3.9 $^{+0.5}_{-0.6}$	1.07 $^{+0.10}_{-0.11}$	8.3	8.3	23.0 $^{+1.4}_{-1.5}$	3	-	-
SDSS J1343-41	132	1.3	10.8 $^{+0.7}_{-0.8}$	5.6 $^{+0.7}_{-0.8}$	2.09 $^{+0.10}_{-0.11}$	13.2	13.2	14.5 $^{+0.8}_{-0.9}$	1	-	-
SDSS J1341-34	141	1.1	11 $^{+1}_{-1}$	5.7 $^{+0.7}_{-0.8}$	1.09 $^{+0.10}_{-0.11}$	12.3	12.3	18.1 $^{+1.0}_{-1.1}$	3	-	-
SDSS J2-11-01	161	1.9	13.3 $^{+0.8}_{-0.9}$	7.3 $^{+0.9}_{-1.0}$	2.86 $^{+0.10}_{-0.11}$	16.2	16.2	14.4 $^{+0.8}_{-0.9}$	3	-	-

18) <http://www.astronomy.wisc.edu/~dave/gravlens/>, accessed on 11/20/2008. See also <http://www.astronomy.wisc.edu/~dave/gravlens/> for details. 19) <http://www.astronomy.wisc.edu/~dave/gravlens/>, accessed on 11/20/2008. See also <http://www.astronomy.wisc.edu/~dave/gravlens/> for details. 20) <http://www.astronomy.wisc.edu/~dave/gravlens/>, accessed on 11/20/2008. See also <http://www.astronomy.wisc.edu/~dave/gravlens/> for details. 21) <http://www.astronomy.wisc.edu/~dave/gravlens/>, accessed on 11/20/2008. See also <http://www.astronomy.wisc.edu/~dave/gravlens/> for details.

19) <http://www.astronomy.wisc.edu/~dave/gravlens/>, accessed on 11/20/2008. See also <http://www.astronomy.wisc.edu/~dave/gravlens/> for details. 20) <http://www.astronomy.wisc.edu/~dave/gravlens/>, accessed on 11/20/2008. See also <http://www.astronomy.wisc.edu/~dave/gravlens/> for details. 21) <http://www.astronomy.wisc.edu/~dave/gravlens/>, accessed on 11/20/2008. See also <http://www.astronomy.wisc.edu/~dave/gravlens/> for details.

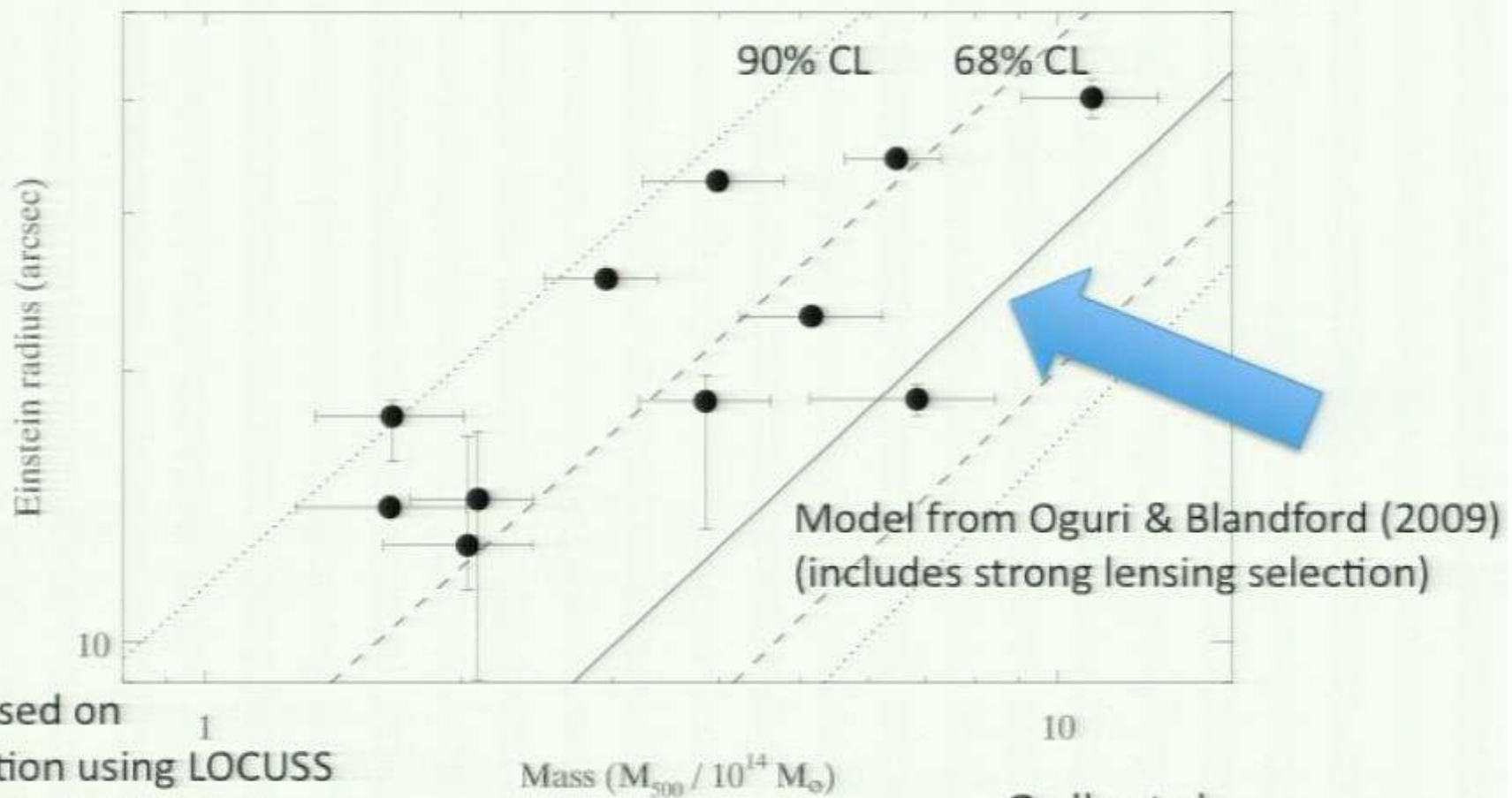
Strong Lensing Cluster Sample

Name	Cluster z^1	r_{500} (")	Y_{500} (10^{-5} Mpc^2)	M_{500} $\times 10^{14} M_{\odot}$	Arc z^1	θ_E (")	θ_S for $(z_l, z_s) = (0.5, 2.0)$ (")	Lensing Ref. ²
Abell 1689	0.18	503	$24.8^{+0.7}_{-1.9}$	$10.9^{+2.1}_{-1.9}$	1.100	42.6	40.2 ± 2.0	1
					3.000	52.3		
					4.800	54.4		
Abell 1703	0.28	251	$4.6^{+1.1}_{-0.4}$	3.9 ± 0.7	0.880	19.2	32.5 ± 1.9	2
					3.380	31.3		
Abell 963	0.21	321	$4.4^{+1.1}_{-0.8}$	$3.9^{+0.7}_{-0.6}$	0.771	6.7	$18.5^{+2.3}_{-6.2}$	3
					1.958	16.5		
RCS1 J2319	0.90	85	$1.5^{+0.6}_{-0.5}$	2.0 ± 0.4	3.860	12.9	$12.8^{+4.7}_{-2.0}$	3
RCS2 J0327	0.56	133	$2.8^{+0.4}_{-0.5}$	2.7 ± 0.4	1.701	21.8	25.3 ± 1.5	4
RCS2 J2327	0.70	155	12.3 ± 0.7	6.5 ± 0.8	1.415	25.9	$34.4^{+2.8}_{-2.1}$	3
					2.983	39.6		
SDSS J1209+26	0.56	161	$7.3^{+0.4}_{-1.9}$	$4.9^{+1.1}_{-1.0}$	1.018	8.3	23.0 ± 1.4	3
					3.949	27.3		
SDSS J1343+41	0.42	134	$0.9^{+0.4}_{-0.3}$	1.6 ± 0.4	2.090	15.2	$14.1^{+1.2}_{-0.9}$	5
					5.200	20.9		
SDSS J1531+34	0.34	164	$1.1^{+0.3}_{-0.2}$	$1.7^{+0.4}_{-0.3}$	1.096	12.3	$18.0^{+2.0}_{-1.8}$	3
SDSS J2111-01	0.64	109	$2.3^{+0.3}_{-0.4}$	2.3 ± 0.4	2.861	16.2	$14.4^{+3.5}_{-6.0}$	3

NOTE.—¹ Cluster and arc redshift references are Limousin et al. (2007, 2008) for Abell 1689; Abell 1703 respectively; Smith et al. (2005) for Abell 963; Gibbank et al. (2008) for RCS1 J2319; Wuyts et al. (2010) for RCS2 J0327; and information on RCS2 J2327 will be published in Gladders et al. (in preparation). All other cluster and arc redshifts are published in Bayliss et al. (2010b).

² Lens model references are: [1] Limousin et al. (2007); [2] Limousin et al. (2008); [3] Sharon et al. in prep; [4] Wuyts et al. (2010); [5] Bayliss et al. (2010a).

Projected Concentrations: Einstein Radius vs. M_{500}



$Y_{SZ} \rightarrow M$ based on scaling relation using LOCUSS
 Weak lensing: Okabe et al.

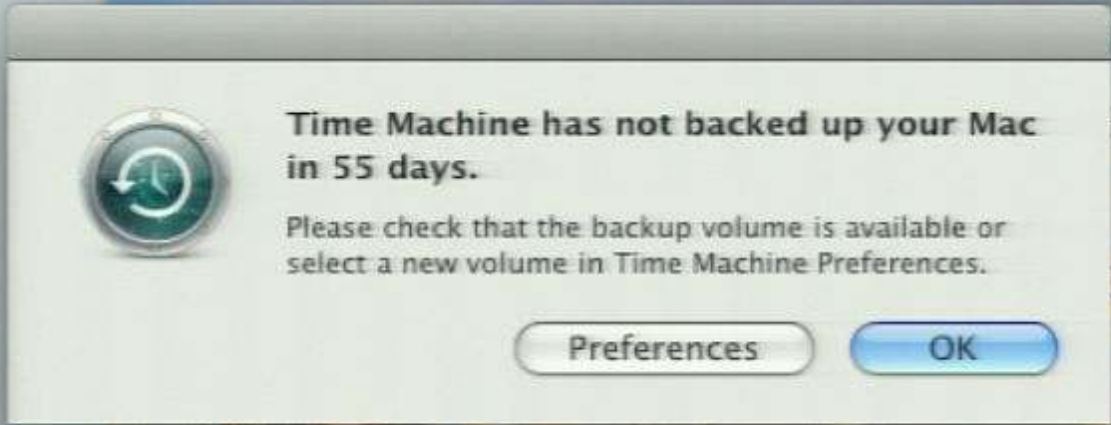
SZ: Marrone et al.

Gralla et al.

arXiv:1011.6341

Moving beyond spherical profiles...

- Simulated dark matter halos are seen to be triaxial (Jing & Suto 2002)
- Simulations suggest that strong lensing clusters should be elongated along the line of sight (e.g., Hennawi et al. 2007)
- The statistical distribution of image locations and types provides information on the dark matter distribution. Baryon cooling tends to make halos more spherical, particularly in the inner regions. Measuring the shapes through different observables (SZ, lensing and BCGs) probes the shape at a range of scales.



Time Machine has not backed up your Mac in 55 days.

Please check that the backup volume is available or select a new volume in Time Machine Preferences.

Preferences OK



Megan Gralla
University of Chicago

Click to add notes

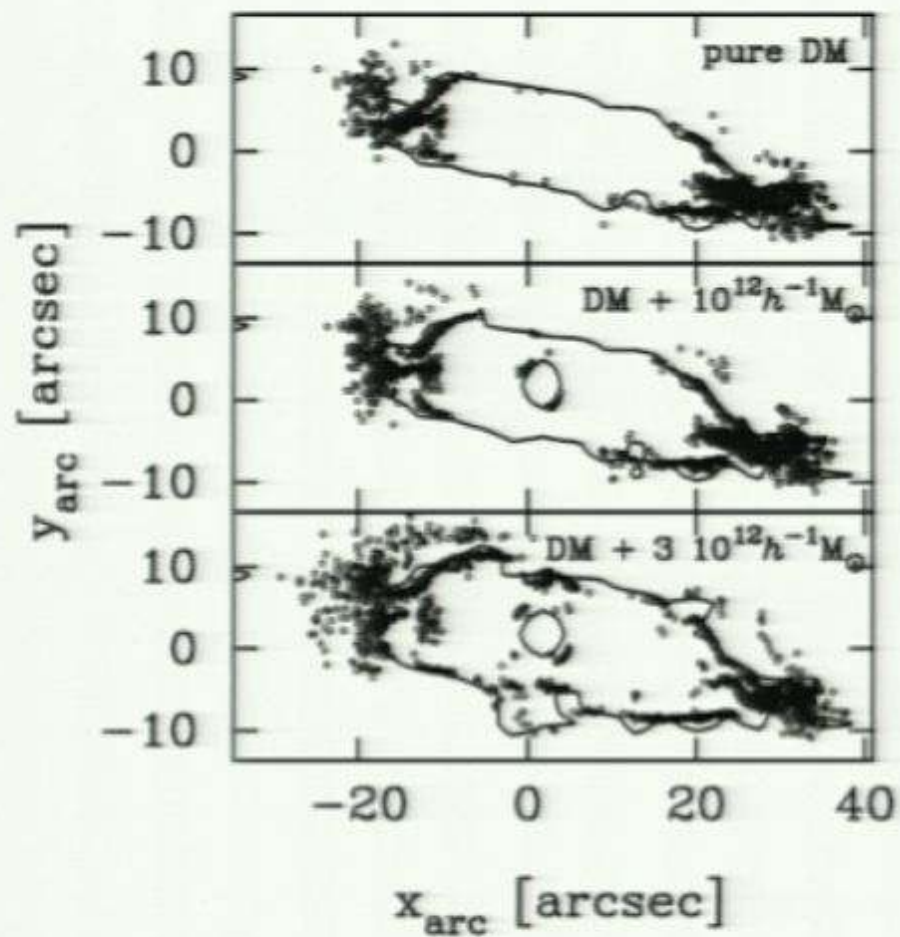
Moving beyond spherical profiles...

- Simulated (Jing & Su)
- Simulation be elongated (al. 2007)
- The statistical distribution of image locations and types provides information on the dark matter distribution. Baryon cooling tends to make halos more spherical, particularly in the inner regions. Measuring the shapes through different observables (SZ, lensing and BCGs) probes the shape at a range of scales.



Moving beyond spherical profiles...

- Simulated dark matter halos are seen to be triaxial (Jing & Suto 2002)
- Simulations suggest that strong lensing clusters should be elongated along the line of sight (e.g., Hennawi et al. 2007)
- The statistical distribution of image locations and types provides information on the dark matter distribution. Baryon cooling tends to make halos more spherical, particularly in the inner regions. Measuring the shapes through different observables (SZ, lensing and BCGs) probes the shape at a range of scales.

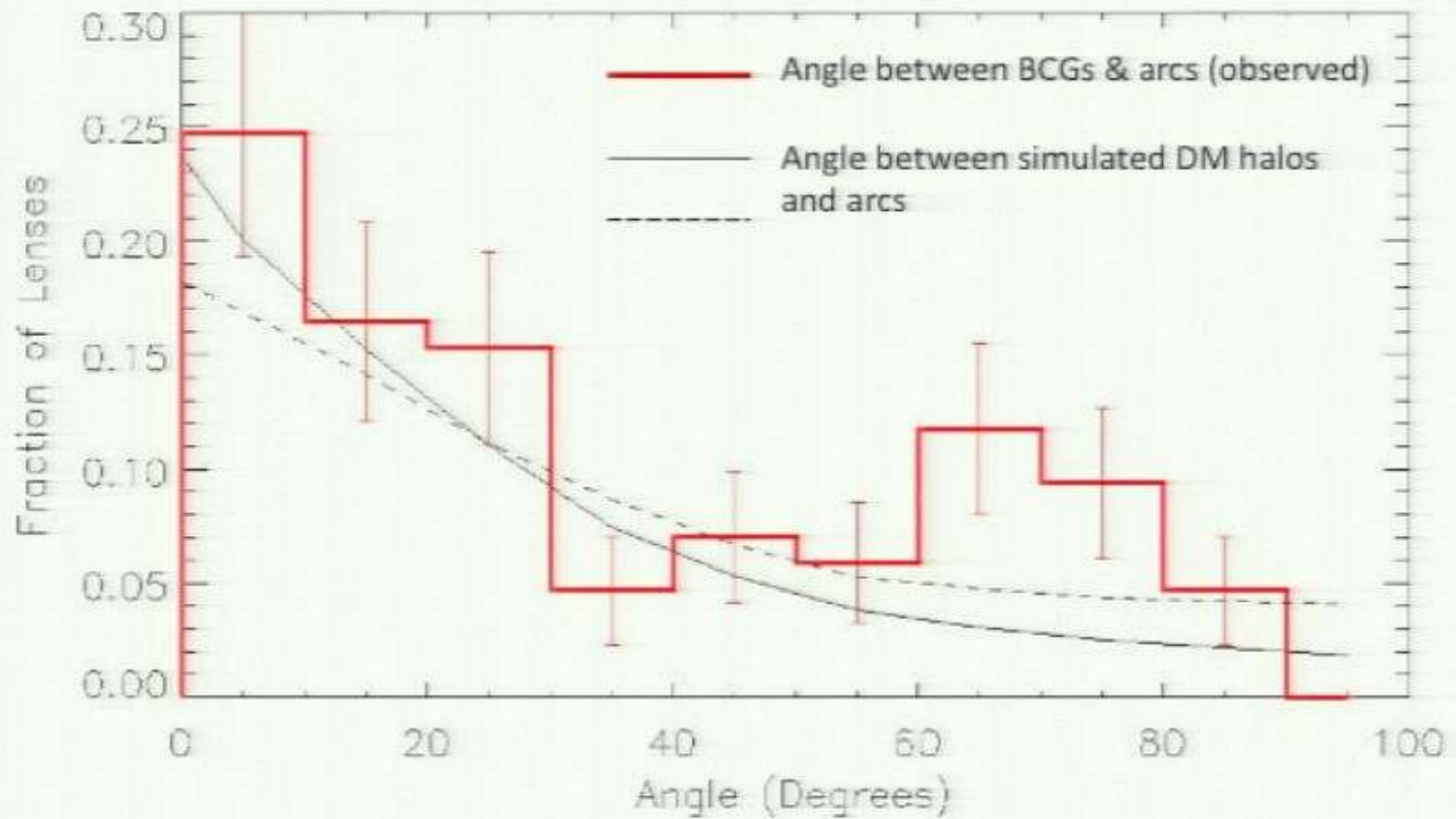


Predictions for the Locations of Lensed Images

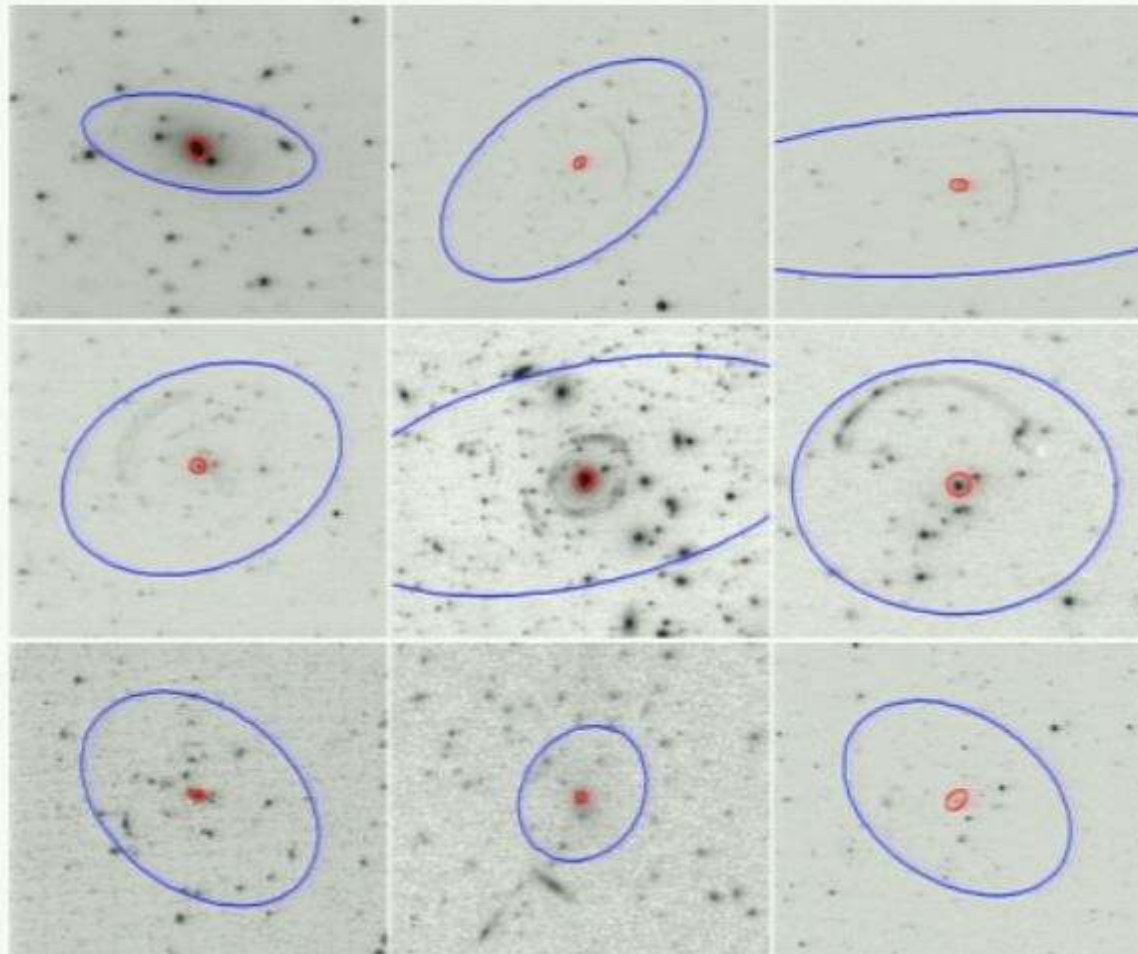
Dalal, Holder & Hennawi 2004

FIG. 7.—Angular distribution of giant arcs for one cluster projection. The panels correspond, from top to bottom, to results from the DM simulation with added central point masses of 0 , $10^{12} h^{-1} M_{\odot}$, and $3 \times 10^{12} h^{-1} M_{\odot}$, respectively. The solid lines are for the critical curves, and symbols show the centers of giant arcs produced in the Monte Carlo simulation.

Arc alignment



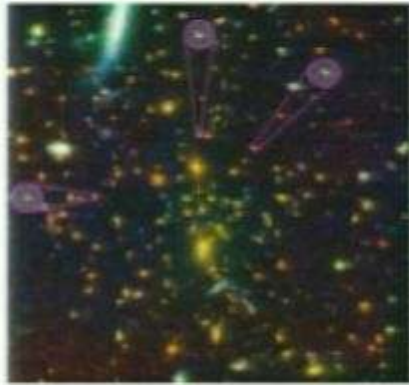
SZ shapes



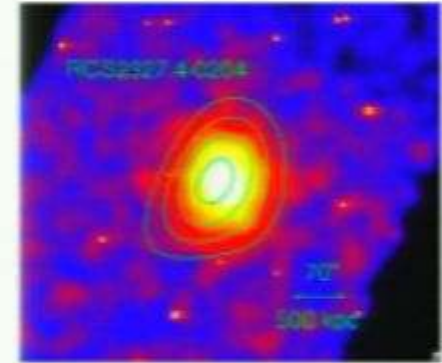
Blue: SZ shape
Red: BCG shape

Tally:

# of BCG/lens aligned	# of SZ/lens aligned	# with BCG, SZ & lens aligned
7	6	6



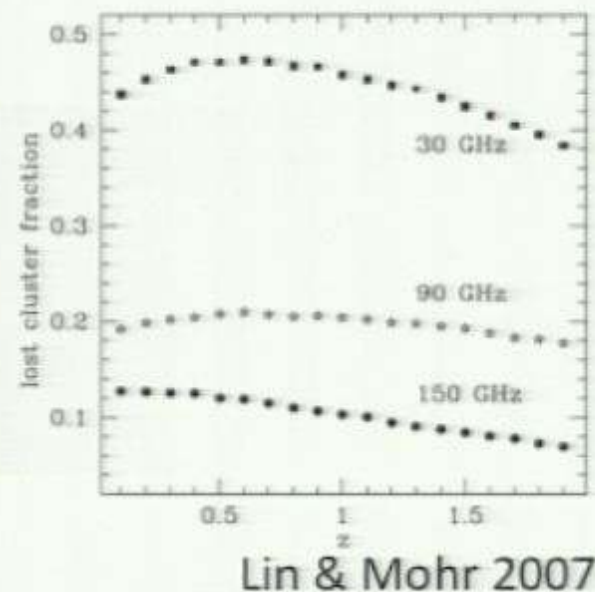
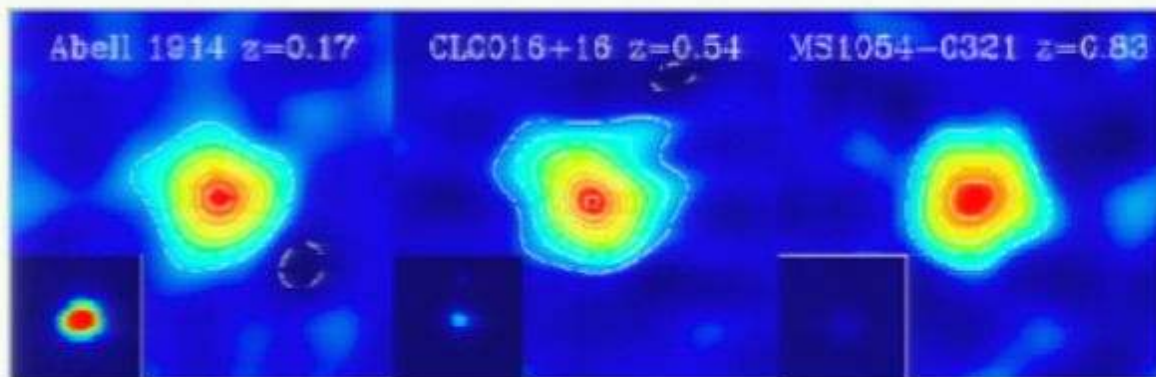
RCS2327 ("ubercluster")



- Combining SZ and X-ray allows the measurement of line of sight elongation (because of their different dependencies on density), which for RCS2327 is 1.3 ± 0.2
- The plane of sky elongation for this cluster is more like 2:1, so the major axis is not aligned along the line of sight. Theory suggests that strong lensing clusters with such large Einstein radii are preferentially aligned along the line of sight.

Radio Sources in Galaxy Clusters: Contaminant for SZ surveys

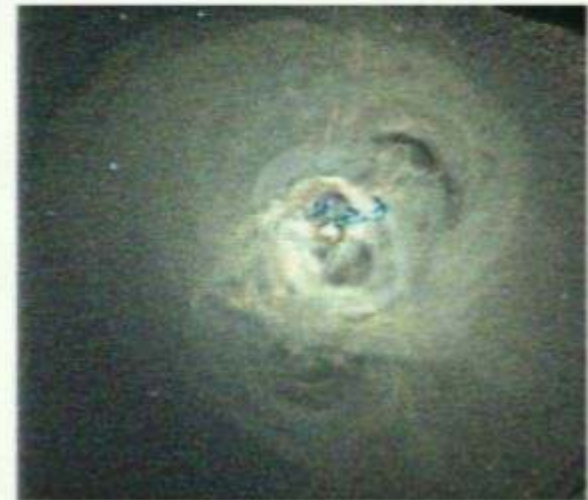
- One motivation for conducting surveys of the SZ effect to find galaxy clusters is its redshift independence



- Radio sources can contaminate the SZ signal, filling in the decrement (Lin & Mohr 2007)

Radio Sources in Galaxy Clusters: Feedback mechanism

- Feedback from radio-loud active galactic nuclei (AGN) is one mechanism invoked to explain the X-ray properties of clusters (for a review see McNamara & Nulsen 2007)
- Studies (e.g., Burns 1990, Eilek 2004, & Mittal et al. 2009) find that most and maybe all galaxy clusters with cool cores also contain radio AGN



Chandra X-ray image of Perseus cluster (Fabian et al. 2006). Two inner cavities contain active radio lobes

Project 2: Radio Sources in Galaxy Clusters

- In order to understand the effect of radio AGN on SZ surveys and on the intracluster gas, we first need to know how the population depends on the cluster mass and redshift
- Previous studies have utilized large samples of nearby clusters (Lin & Mohr 2007; Croft, deVries & Becker 2007; Best et al. 2007) to explore the cluster radio source population, or in-depth observations of smaller samples of more distant clusters (Stocke et al. 1999; Branchesi et al. 2006) to constrain the redshift evolution of this population.
- With the advent of uniformly selected, comprehensive surveys spanning a wide redshift range, we can address this problem statistically

Red-Sequence Cluster Surveys

- RCS-1 (Gladders & Yee 2005)
 - two-band (R_c and z') optical survey at CFHT and CTIO uses red sequence cluster finding methods
 - well-defined sub-sample of $\sim 1,000$ clusters (see Gladders et al. 2007)
 - significance > 3.3 , $0.35 < z < 0.95$, red galaxy richness $B_{gc} > 300$ (Abell richness class 0 $\sim B_{gc} 600$), richness errors $< 50\%$
- RCS-2 (Gilbank et al. arXiv:1012.3470)
 - three-band (g', r', z') optical survey at CFHT using Megacam. Uses red sequence cluster finding methods
 - Survey data acquisition is complete
 - Analysis still underway. Total area $\sim 1,000$ square degrees

FIRST survey

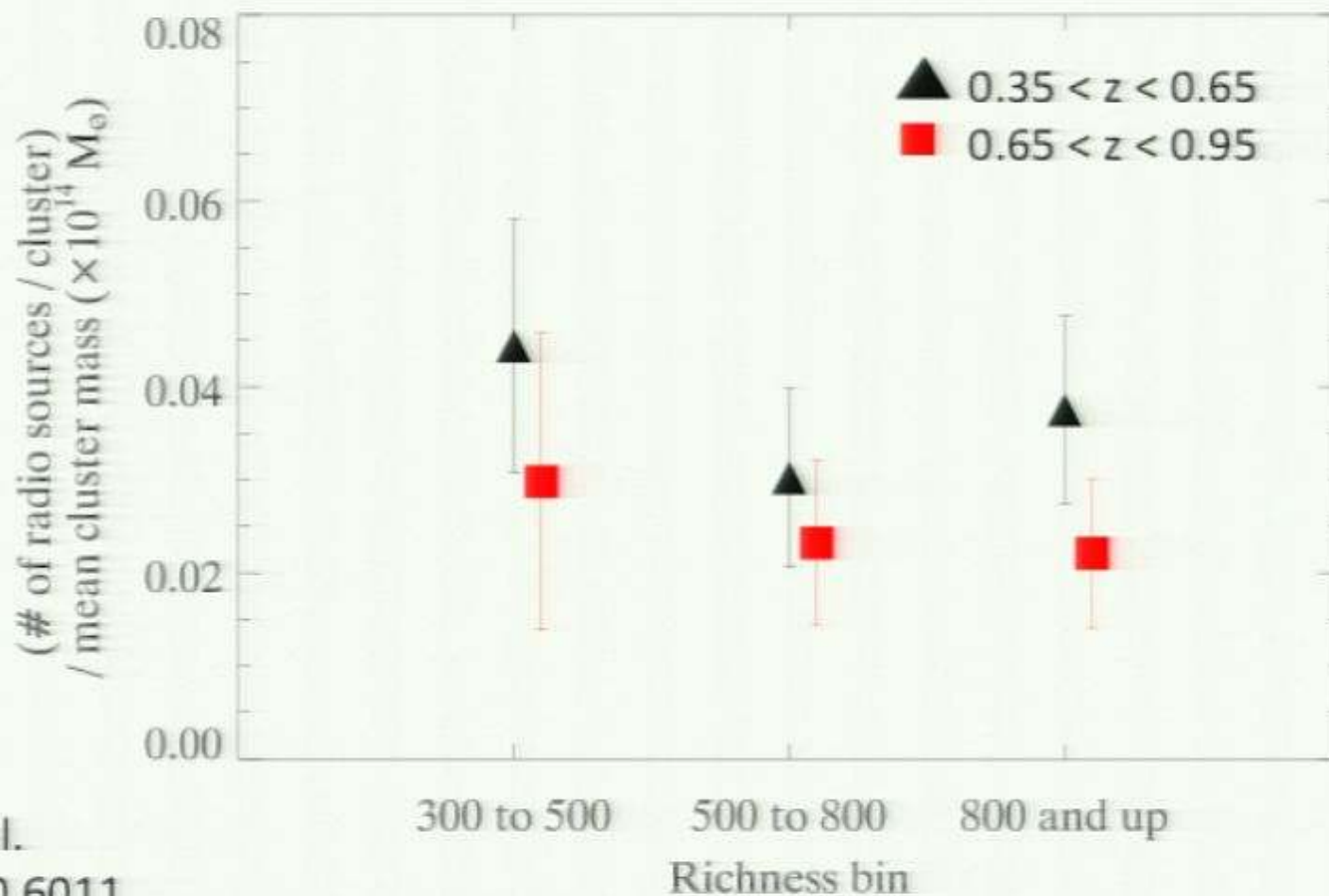
References: Becker, White & Helfand 1995

White, et al. 1997

- VLA B-array, 1.4 GHz resolution $\sim 5''$
- 10,000 square degrees
- sensitivity limit ~ 1.0 mJy



Radio sources / cluster / unit mass



Gralla et al.

arXiv:1010.6011

Pirsa: 11010106

Page 36/43

Implications

- The number of radio sources (with $L_{1.4\text{GHz}} > 4.1 \times 10^{24} \text{ W Hz}^{-1}$) per $10^{14} M_{\odot}$ of cluster mass is 0.031 ± 0.004 .
- This result has informed recent predictions for SZ survey contamination (Lin et al. 2009)
- Studies of X-ray and IR AGN see dramatic redshift evolution in the cluster AGN population over the same redshift range (e.g., Martini, Sivakoff, & Mulchaey 2009 and Krick et al. 2009). This may indicate two separate populations, or evolution between different modes of activity (such as proposed by Hickox et al. 2009).

For comparison, X-ray AGN evolution

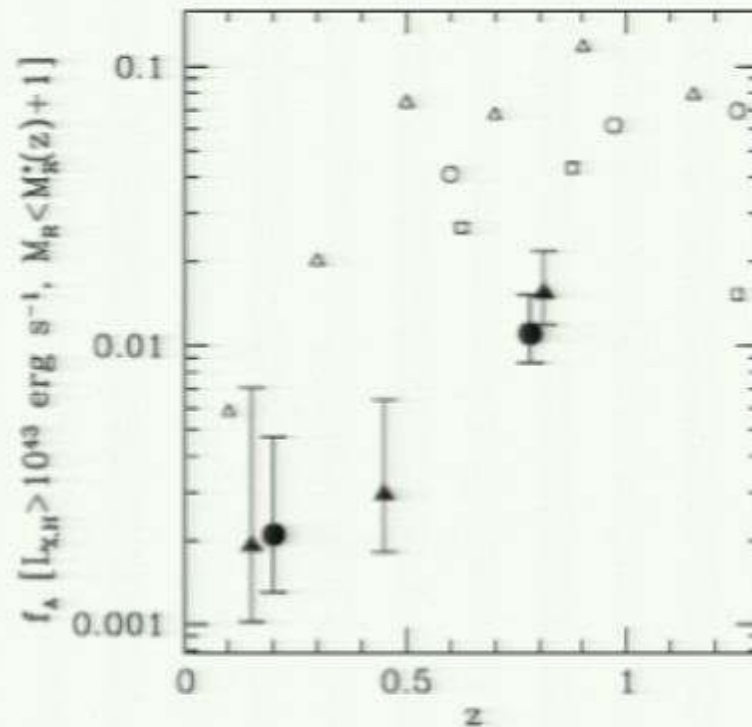
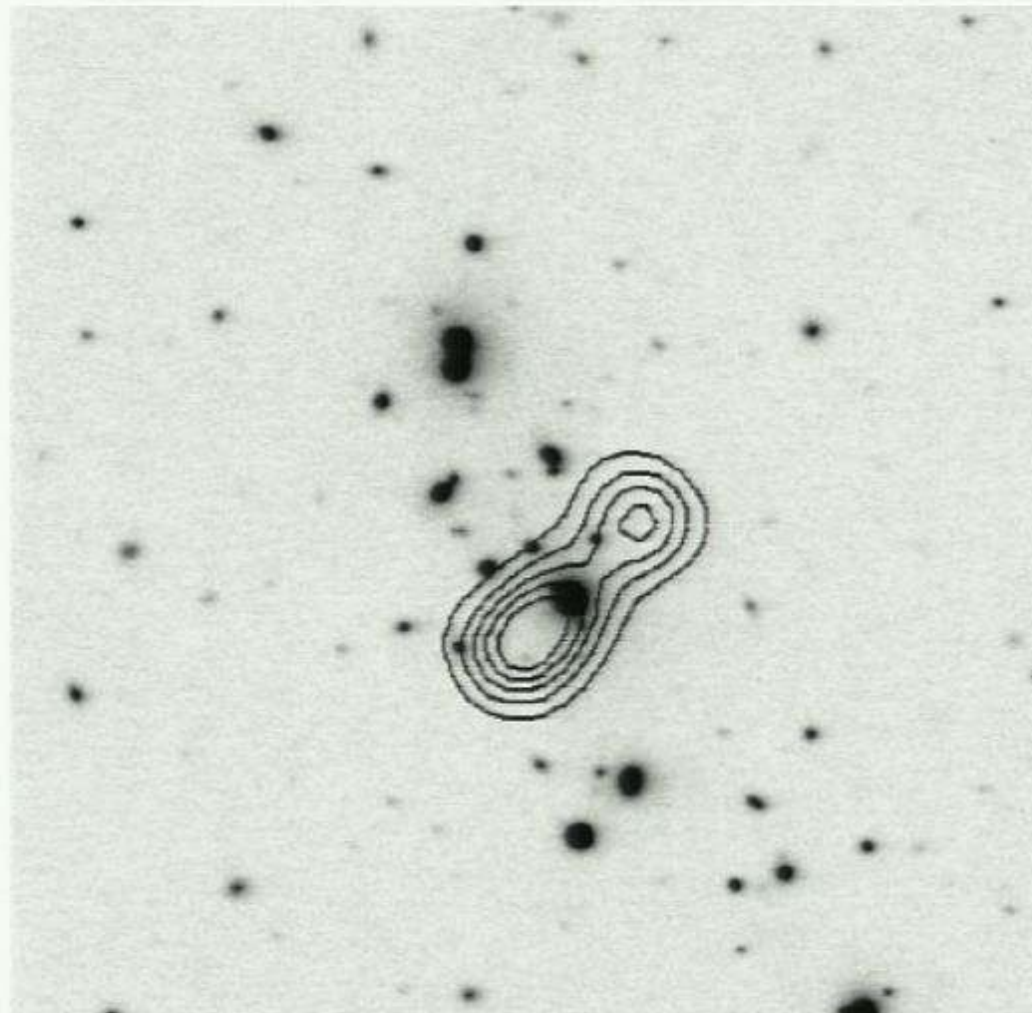


FIG. 3.— Evolution of the AGN population in clusters from $z = 0$ to $z = 1.3$ (filled symbols). The fraction of cluster members more luminous than $M_R^* + 1$ with AGN that have $L_{X,R} > 10^{43} \text{ erg s}^{-1}$ is shown in two redshift bins ($z < 0.4$, $z > 0.4$; filled circles) and three redshift bins ($z < 0.3$, $0.3 < z < 0.8$, $0.8 < z < 1.3$; filled triangles). We also show our estimate of the field AGN fraction based on the galaxy LF estimates by Ilbert et al. (2005, open triangles), Dahlen et al. (2005, open circles), and Chen et al. (2003, open squares). See §4.4 for further details.

Characterizing the sample

FIRST radio contours over RCS1 images



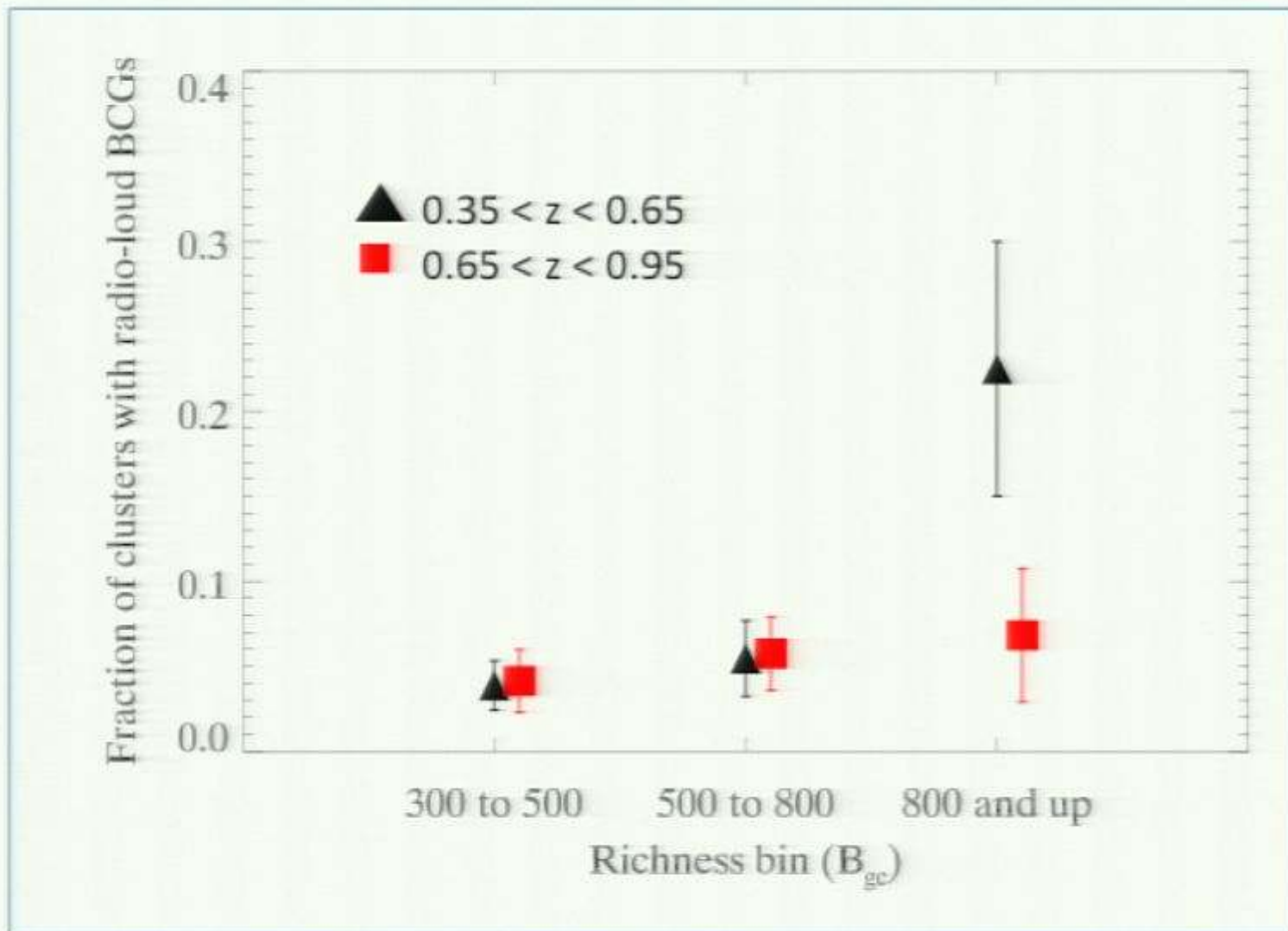
132655+302112

$z \sim .37$

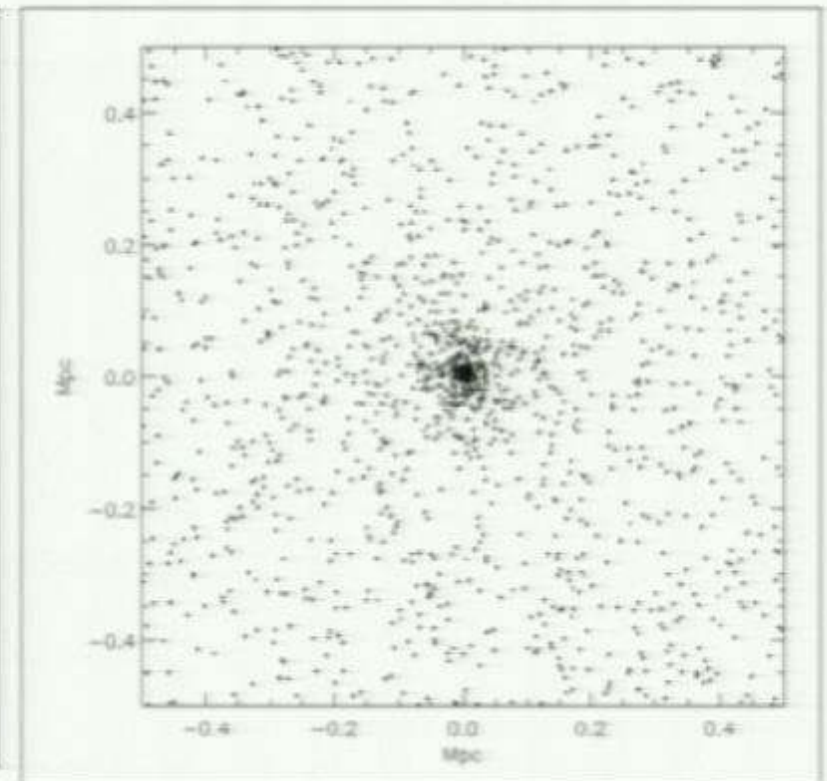
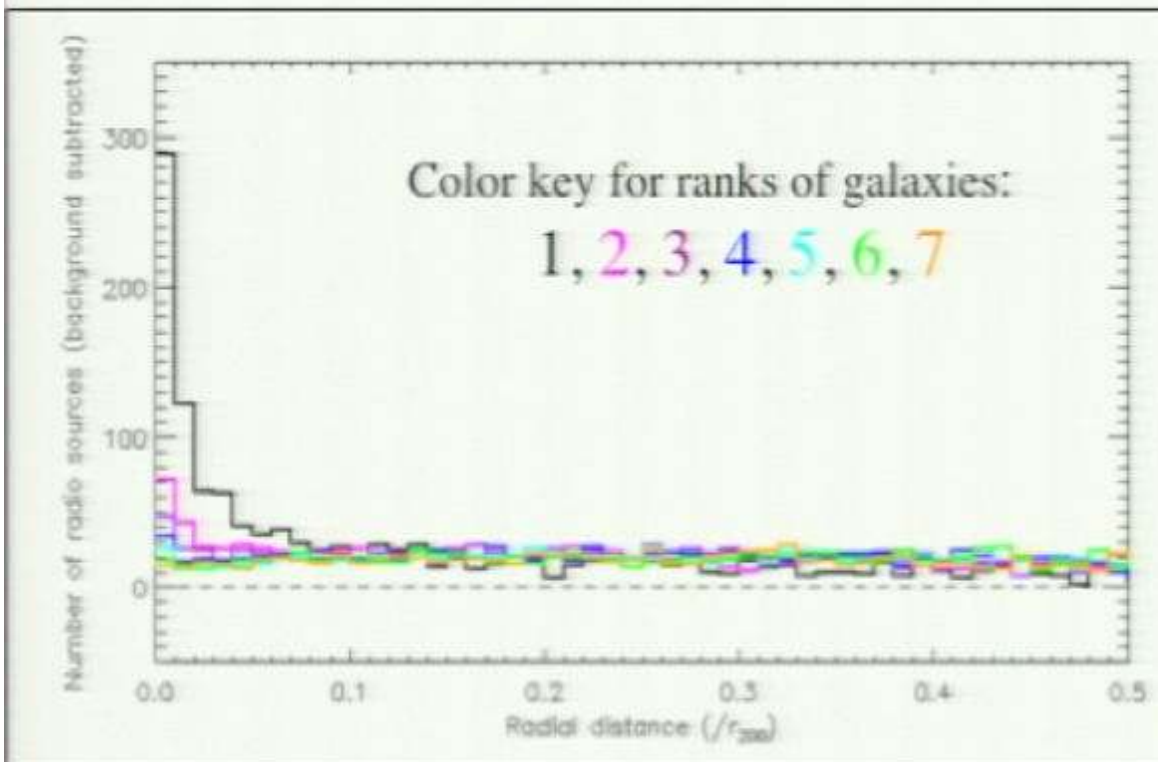
$B_{gc} 1425$

Page 39/43

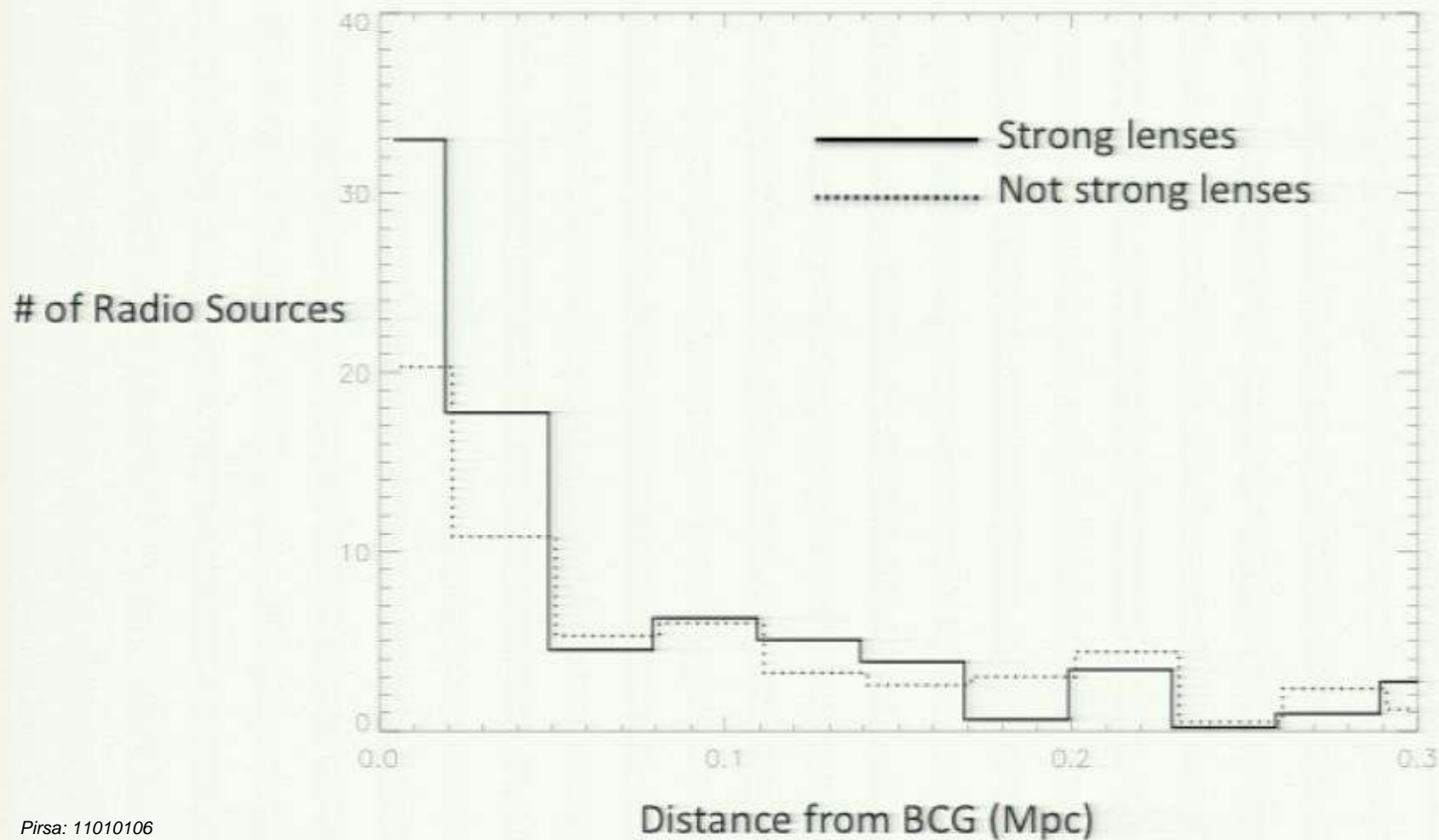
Radio-loud BCGs



Radio Sources in galaxy clusters from RCS2



Radio AGN Activity in Strong Lensing Clusters



Conclusions

- The number of radio sources (with $L_{1.4\text{GHz}} > 4.1 \times 10^{24} \text{ W Hz}^{-1}$) per $10^{14} M_{\odot}$ of cluster mass is 0.031 ± 0.004 over a wide redshift range (0.35 to 0.95) \rightarrow good news for SZ surveys!
- One exception to this constant is that the fraction of clusters with radio-loud BCGs is higher (at 2σ) in the low redshift (<0.65) richest clusters. We will investigate this more with RCS2
- Strong lensing galaxy clusters tend to have larger Einstein radii for a given mass (as measured by SZ) than expected from theory
- The BCG is frequently aligned with the SZ, and images tend to form at the projected major axes

